# Monitoring methylation-driven genes as prognostic biomarkers for cervical cancer

BEI LIU[1], YUJUN LI[2], HANYU LIU[3], TIANSHUO ZHAO[3], BINGFENG HAN[3], QINGBIN LU[1] and FUQIANG CUI[1]

[1]Department of Laboratorial Science and Technology, School of Public Health, Peking University, Beijing 100191; [2]Department of Pathology, The Affiliated Hospital of Qingdao University, Qingdao, Shandong 266003; [3]Department of Epidemiology and Biostatistics, School of Public Health, Peking University, Beijing 100191, P.R. China

Received July 8, 2021; Accepted May 24, 2022

DOI: 10.3892/ije.2022.11

**Abstract.** Aberrant DNA methylations are markedly associated with the development of cervical cancer (CC); however, only a limited number of studies have focused on identifying the DNA methylation-driven genes in CC by integrative bioinformatics analysis to predict the prognosis of CC. In the present study, DNA methylation and transcriptome profiling data were downloaded from The Cancer Genome Atlas database. DNA methylation-driven genes were obtained using the MethylMix R package. The Database for Annotation, Visualization and Integrated Discovery and ConsensusPathDB were used to perform Gene Ontology and pathway analyses, respectively. The survival R package was used to analyze overall survival rates associated with methylation-driven genes. In total, data for 125 methylation-driven mRNAs and 38 methylation-driven long-coding RNAs (lncRNAs) were obtained. Based on the univariate and multivariate Cox regression models, it was demonstrated that FLT1 (fms-related tyrosine kinase 1) mRNA, MKI67 (marker of proliferation Ki-67), PLEKHG6 (pleckstrin homology domain containing family G with RhoGef domain member 6) and POLE2 (DNA polymerase epsilon 2) lncRNAs were predictors of the overall survival of patients with CC. According to DNA methylation and gene expression, FLT1 mRNA, and the MKI67, PLEKHG6 and POLE2 lncRNAs functioned as independent biomarkers for the prognosis of CC. DNA methylation assays revealed that the promoter methylation levels of FLT1 were significantly upregulated in CC and cervical adenocarcinoma compared with normal controls. The results of immunohistochemical analysis revealed that the expression level of FLT1 in CC tissues was higher than that in normal tissues; however, the PLEKHG6 gene was expressed at high levels in normal tissues. On the whole, the present study demonstrates that methylation-driven lncRNAs and mRNAs contribute to the survival of patients with CC, and FLT1 mRNA, and the MKI67, PLEKHG6 and POLE2 lncRNAs may be potential biomarkers for the prognosis of CC.

## Introduction

Cervical cancer (CC) is an extremely common malignant tumor of the female reproductive system, and the prevalence of CC is the second highest in the whole category of female malignant tumors (1,2). Data on global cancer epidemics from the International Cancer Research Agency have demonstrated that the year 2020 witnessed almost 600,000 CC cases and 34,000 deaths resulted from this disease (3,4). Currently applied vaccines, which are essentially focusing on prophylaxis, cannot combat the immense numbers of patients with CC worldwide (5). Patients with CC present no notable differences on clinical outcomes. Therefore, it is difficult to predict the disease at the early stage. As a result of the heterogeneity of CC, the successful development of individual-based treatments is a difficult task (6). Therefore, the exploration of potential and effective biomarkers which may be used to diagnose and predict the prognosis of patients with CC is of utmost urgency (7).

The aberrant DNA hypermethylation of CpG island (CGI) promoters (promoter hypermethylation) occurs in numerous types of cancer (8). CGIs are contiguous groups of dinucleotides mainly located at the 5' end of a gene and are characterized by a high guanine-cytosine (GC) content. CGI hypermethylation has been recognized as one of the key features of cancer (9). The increased DNA methylase activity in tumor cells or the destruction of CGI local protection mechanisms leads to genomic instability, transposon reactivation, chromosome structural changes and the activation of cancer-related genes,

*Correspondence to:* Professor Fuqiang Cui or Dr Qingbin Lu, Department of Laboratorial Science and Technology, School of Public Health, Peking University, 38 Xueyuan Road, Haidian, Beijing 100191, P.R. China
E-mail: cuifuq@126.com
E-mail: qingbinlu@bjmu.edu.cn

*Key words:* cervical cancer, methylation-driven mRNA, methylation-driven lncRNA, biomarkers, overall survival rate

etc. (10,11). DNA hypermethylation causes the silencing of cancer-related genes, such as genes related to apoptosis, cell cycle regulation and angiogenesis (12); this promotes the incidence and development of cancer. CGIs in the promoter region of genes are under abnormal methylation, which induces the transcriptional silencing of tumor suppressor genes and carcinogenesis (10,13). It has been reported that DNA methylation occurs in 70-100% of CC cases, as well as in 30-80% of cervical precancerous lesions (14). To date, >100 genes, which have been found to be methylated or silenced in CC, may be applied as latent biological markers for the prediction of CC (15).

Methylation-driven genes are directly responsible for carcinogenesis and are closely related to the transformation, development and invasion of cancer (16). DNA methylation alterations of driver genes can alter the expression of cognate genes, interacting genes and genes in the same downstream pathways, subsequently causing inference in cancer-related pathways and inducing the cancer phenotype. The downregulated expression of SFRP1 by promoter hypermethylation has been previously demonstrated to result in the constitutive activation of the Wnt pathway, which in turn contributes to colorectal cancer malignancy (17). Studies on prostate cancer have demonstrated that the hypomethylation of promoter regions of the Wnt5b gene upregulate gene expression, eventually contributing to prostate cancer progression (18,19). Guo *et al* (20) reported that the detection of the methylation frequencies of SLC19A1, CREB and CYLD could be used to predict the recurrence of colorectal cancer. To date, several studies have been conducted to identify DNA methylation-driven genes using the MethylMix algorithm and The Cancer Genome Atlas (TCGA) database (21-23). However, only a limited number of studies have focused on assessing methylation-driven genes in CC. A previous study merely attained the information on mRNAs based on methylation, which can predict the prognosis of CC (24).

The present study identified hypomethylated and hypermethylated genes associated with specific diseases in order to obtain CC-specific long-coding RNA (lncRNA) sequences driven by methylation, and that may be used to predict the diagnosis and prognosis of patients with CC. These findings may provide new insight into the prediction of the prognosis of patients with CC, using the combination of methylation-driven lncRNAs and mRNAs.

## Materials and methods

*Data retrieval and integrative analysis*. RNA-sequencing data from 310 cases (255 cervical squamous cell carcinoma, 31 cervical adenocarcinoma, 17 cervical mucinous cystic neoplasms, 4 cervical intraepithelial neoplasia and 3 normal cervical tissues), DNA methylation data from 313 cases (257 cervical squamous, 32 cervical adenocarcinoma, 17 cervical mucinous cystic neoplasms, 4 cervical intraepithelial neoplasia and 3 normal cervical tissues) were obtained from TCGA database (https://portal.gdc.cancer.gov/). The acquisition of DNA methylation data was implemented on the Illumina Infinium Human Methylation 450 platform. Above all, all retrieved data were analyzed and normalized to obtain access to differentially expressed genes (DEGs) and differentially methylated genes (DMGs), and the analytical procedures were performed on the Limma package of R software (version 3.6.2, Mathsoft, Inc.). The DEGs and DMGs were then integrated for analysis using R-software based on the MethylMix algorithm (version 3.6.2, Mathsoft, Inc.). The missing values and the matched intersecting methylation DNA data were filtered with the RNA expression data. A total of 306 samples of patients with CC and three samples of non-CC patients were recruited for the next calculation step. Subsequently, the correlation between the methylation level and gene expression was calculated. The Wilcoxon rank sum test to calculate the differences in methylation between the CC patient samples and adjacent non-CC patient samples. Pearson's correlation analysis was then used to determine the correlation between the methylation level and gene expression. Finally, the final output of MethyMix included genes with both transcriptional predictability and a differential methylation status. Finally, mRNAs and lncRNAs driven by methylation were acquired.

*Functional enrichment analysis on methylation-driven genes*. In addition to an open source platform (https://david.ncifcrf.gov/), the Database for Annotation, Visualization and Integrated Discovery (DAVID) was used to explore the functions of methylation-driven mRNAs. Gene Ontology (GO) analysis of methylation-driven genes were visualized by 'GOplot' R package. Subsequently, the Kyoto Encyclopedia of Genes and Genomes (KEGG) analysis was also used to perform the pathway enrichment analysis for those DNA methylation-driven genes through KOBAS 3.0 (http://kobas.cbi.pku.edu.cn). A value of $P<0.05$ was set as the cut-off standard.

*Construction of prognostic signatures*. Univariate Cox regression analysis was conducted to determine the association between the expression of DNA methylation-driven genes and the prognosis of patients with CC. Genes with a P-value <0.05 were regarded as prognostic methylation-driven genes and were subsequently fitted into the multivariate Cox regression analysis. A DNA methylation-driven gene-based prediction model was constructed using the linear combination of the expression levels of methylation-driven genes with coefficients (β) calculated from multivariate Cox regression as the weights. The risk score for each patient was calculated based on the following risk score formula: Risk score=expression of gene1 x β1 + expression of gene2 x β2 + …expression of genen x βn. Subsequently, patients were divided into the high- and low-risk groups by setting the median value of risk scores as the cut-off value. The overall survival (OS) of these two groups was calculated using the Kaplan-Meier method with the log-rank test. Receiver operating characteristic (ROC) curves were used to assess the predictive performance of the prognostic model and area under the curve (AUC) values were calculated. The expression patterns of DNA methylation-driven genes in this prognostic model were visualized using the 'pheatmap' R package (R software3.6.2, Mathsoft, Inc.).

*Survival analysis*. In order to perform an in-depth assessment of methylation-driven genes associated with prognosis and

Table I. Methylation-driven mRNAs.

| Gene | Normal mean | Tumor mean | logFC | P-value | FDR |
|---|---|---|---|---|---|
| OTX1 | 0.008609738 | 2.422484869 | 8.136302547 | 0.002907656 | 0.048976629 |
| HIST1H2AM | 0.01357165 | 1.050542267 | 6.274394268 | 0.002969844 | 0.048976629 |
| KREMEN2 | 0.025207773 | 5.182757296 | 7.683707338 | 0.002907656 | 0.048976629 |
| HIST1H2BH | 0.025716823 | 5.936443692 | 7.850742668 | 0.002907656 | 0.048976629 |
| POLQ | 0.03518915 | 3.045189881 | 6.435257713 | 0.002907656 | 0.048976629 |
| CLSPN | 0.03697982 | 3.388624708 | 6.517817854 | 0.002907656 | 0.048976629 |
| MCM10 | 0.052274933 | 4.303523361 | 6.363255173 | 0.002907656 | 0.048976629 |
| CCDC150 | 0.05328457 | 0.70413694 | 3.724066303 | 0.002969847 | 0.048976629 |
| AL109811.2 | 0.058717813 | 1.204383547 | 4.358352852 | 0.002969847 | 0.048976629 |
| ASPM | 0.06079877 | 5.853531897 | 6.589121431 | 0.002907656 | 0.048976629 |
| CKAP2L | 0.060848407 | 4.653990218 | 6.257104882 | 0.002907656 | 0.048976629 |
| E2F8 | 0.070134097 | 5.908846804 | 6.396616784 | 0.002907656 | 0.048976629 |
| E2F2 | 0.07500838 | 6.683604622 | 6.477430797 | 0.002907656 | 0.048976629 |
| KIF18B | 0.094850093 | 9.138667451 | 6.590190811 | 0.002907656 | 0.048976629 |
| HASPIN | 0.096249443 | 2.47958553 | 4.687176983 | 0.002969847 | 0.048976629 |
| HIST1H2AG | 0.115060643 | 1.913568162 | 4.055798945 | 0.002969847 | 0.048976629 |
| UHRF1 | 0.124969837 | 11.78907108 | 6.559726315 | 0.002907656 | 0.048976629 |
| TROAP | 0.147849247 | 11.56818612 | 6.289891966 | 0.002907656 | 0.048976629 |
| DLGAP5 | 0.153893317 | 12.06073375 | 6.292243291 | 0.002907656 | 0.048976629 |
| RAD54B | 0.162129053 | 1.128769995 | 2.799536996 | 0.002907656 | 0.048976629 |
| NEK2 | 0.17629113 | 13.32260506 | 6.239772511 | 0.002907656 | 0.048976629 |
| CENPE | 0.1779729 | 3.701522009 | 4.378389124 | 0.002969847 | 0.048976629 |
| PIF1 | 0.22515228 | 3.478096936 | 3.949325149 | 0.002969847 | 0.048976629 |
| KIF24 | 0.2599404 | 2.147583169 | 3.046461223 | 0.002907656 | 0.048976629 |
| DDIAS | 0.284714567 | 2.745727824 | 3.269600411 | 0.002969847 | 0.048976629 |
| ATAD5 | 0.291022067 | 2.476068676 | 3.088850875 | 0.002907656 | 0.048976629 |
| DNA2 | 0.296769 | 3.329539141 | 3.487910197 | 0.002969847 | 0.048976629 |
| ZNF296 | 0.303531533 | 4.707985191 | 3.955191474 | 0.002969847 | 0.048976629 |
| FAM83D | 0.304326433 | 23.02657124 | 6.241536143 | 0.002907656 | 0.048976629 |
| ECE2 | 0.383145467 | 3.429845882 | 3.16217961 | 0.002907656 | 0.048976629 |
| PARPBP | 0.384524433 | 3.276042714 | 3.09080699 | 0.002907656 | 0.048976629 |
| HELLS | 0.3898357 | 5.23057021 | 3.746030111 | 0.002969847 | 0.048976629 |
| SGO2 | 0.412476167 | 3.403119544 | 3.044475165 | 0.002969847 | 0.048976629 |
| FANCD2 | 0.435973233 | 4.350073 | 3.318728143 | 0.002907656 | 0.048976629 |
| RELT | 0.442929167 | 2.479509729 | 2.48490698 | 0.002969847 | 0.048976629 |
| MND1 | 0.504417033 | 6.33443716 | 3.650527537 | 0.002969847 | 0.048976629 |
| BRCA1 | 0.507887067 | 4.548310873 | 3.162751223 | 0.002969847 | 0.048976629 |
| C5orf34 | 0.5172911 | 2.765671281 | 2.418581417 | 0.002907656 | 0.048976629 |
| CENPO | 0.5524477 | 4.275784107 | 2.952279213 | 0.002907656 | 0.048976629 |
| MYBL2 | 0.552865033 | 58.36758471 | 6.72209623 | 0.002907656 | 0.048976629 |
| POLE2 | 0.654987567 | 6.006028095 | 3.196871798 | 0.002907656 | 0.048976629 |
| CENPL | 0.658509633 | 2.976383827 | 2.176284134 | 0.002907656 | 0.048976629 |
| MARVELD2 | 0.671502467 | 5.997847346 | 3.1589802 | 0.002969847 | 0.048976629 |
| CHEK1 | 0.735316333 | 5.703614173 | 2.955439456 | 0.002907656 | 0.048976629 |
| OSBPL3 | 0.741138933 | 6.655781915 | 3.166792243 | 0.002907656 | 0.048976629 |
| WDHD1 | 0.788465033 | 6.624031029 | 3.07059075 | 0.002969847 | 0.048976629 |
| CBX8 | 0.829757267 | 3.313400315 | 1.997551252 | 0.002969847 | 0.048976629 |
| TRAIP | 0.8313529 | 4.403457653 | 2.405103872 | 0.002969847 | 0.048976629 |
| MYO19 | 0.956252333 | 7.737194882 | 3.016347344 | 0.002907656 | 0.048976629 |
| AC145124.1 | 1.017866967 | 0.098647165 | -3.367127609 | 0.002896012 | 0.048976629 |
| NUP210 | 1.106373633 | 19.89151312 | 4.168242439 | 0.002969847 | 0.048976629 |
| RNU6-247P | 1.133219833 | 0.247219555 | -2.196562986 | 0.001125537 | 0.048976629 |

Table I. Continued.

| Gene | Normal mean | Tumor mean | logFC | P-value | FDR |
|---|---|---|---|---|---|
| AC134043.2 | 1.205617333 | 0.104221029 | -3.532053754 | 0.002969788 | 0.048976629 |
| MAP7 | 1.210302133 | 10.97342529 | 3.180574781 | 0.002969847 | 0.048976629 |
| BRI3BP | 1.226047 | 8.72528698 | 2.831188298 | 0.002907656 | 0.048976629 |
| KNSTRN | 1.267626333 | 7.984351493 | 2.655045698 | 0.002907656 | 0.048976629 |
| AC009806.1 | 1.285511 | 0.145998563 | -3.138315879 | 0.002925703 | 0.048976629 |
| POLE | 1.315502 | 6.201415209 | 2.236984045 | 0.002907656 | 0.048976629 |
| TMEM206 | 1.379000333 | 4.893858761 | 1.82734966 | 0.002969847 | 0.048976629 |
| AL133346.1 | 1.434255967 | 0.106993678 | -3.744705055 | 0.002644399 | 0.048976629 |
| ESRP1 | 1.443912813 | 29.74875038 | 4.364773531 | 0.002969847 | 0.048976629 |
| AC112715.1 | 1.4462248 | 0.118338606 | -3.611299114 | 0.002965719 | 0.048976629 |
| CHTF18 | 1.462383 | 9.24523781 | 2.660389225 | 0.002907656 | 0.048976629 |
| ECT2 | 1.4816846 | 22.15220232 | 3.90213985 | 0.002969847 | 0.048976629 |
| MAPK13 | 1.501844767 | 18.86749931 | 3.651095615 | 0.002969847 | 0.048976629 |
| RFTN2 | 1.595348667 | 0.31019602 | -2.362619679 | 0.002969847 | 0.048976629 |
| AC109309.1 | 1.602678533 | 0.104860342 | -3.933944014 | 0.001162976 | 0.048976629 |
| CHAF1B | 1.6720722 | 7.810766497 | 2.223826988 | 0.002969847 | 0.048976629 |
| ZWILCH | 1.708687667 | 8.741075 | 2.354922008 | 0.002907656 | 0.048976629 |
| CHEK2 | 1.774875333 | 6.630946745 | 1.901497175 | 0.002907656 | 0.048976629 |
| INTS7 | 1.820999 | 9.316283118 | 2.355024353 | 0.002907656 | 0.048976629 |
| SIRT7 | 1.844280333 | 6.782226856 | 1.878701077 | 0.002907656 | 0.048976629 |
| AL139339.1 | 1.938017667 | 0.125707253 | -3.946441924 | 0.002879369 | 0.048976629 |
| CHAF1A | 2.076047667 | 16.8995404 | 3.025072538 | 0.002907656 | 0.048976629 |
| RF00265 | 2.089666333 | 0.136408423 | -3.937267965 | 0.001504763 | 0.048976629 |
| NXT2 | 2.091489 | 8.301585023 | 1.988856406 | 0.002907656 | 0.048976629 |
| TMEM252 | 2.106628667 | 0.19583094 | -3.42725541 | 0.002418008 | 0.048976629 |
| DARS2 | 2.133191 | 11.35261951 | 2.411940173 | 0.002907656 | 0.048976629 |
| BAIAP2L1 | 2.15688 | 19.55399884 | 3.180445854 | 0.002969847 | 0.048976629 |
| ABCA9 | 2.19188 | 0.125320954 | -4.128469253 | 0.002907628 | 0.048976629 |
| AC027682.6 | 2.313769 | 0.252232545 | -3.197418496 | 0.002969817 | 0.048976629 |
| AC055874.1 | 2.3517578 | 0.117155321 | -4.327245109 | 0.000133275 | 0.048976629 |
| RNU5B-4P | 2.435468 | 0.157760404 | -3.94839197 | 0.001411833 | 0.048976629 |
| MIR497HG | 2.491191667 | 0.151214923 | -4.042163599 | 0.002969847 | 0.048976629 |
| LINC02310 | 2.498536333 | 0.084457297 | -4.886717316 | 0.001686668 | 0.048976629 |
| AJ011932.1 | 2.579065 | 0.105607893 | -4.61005856 | 0.002370969 | 0.048976629 |
| RF02204 | 2.585491 | 0.113003328 | -4.516001121 | 0.00023333 | 0.048976629 |
| LIG1 | 2.855578 | 17.84753708 | 2.643870302 | 0.002907656 | 0.048976629 |
| DSN1 | 3.161946 | 20.01669406 | 2.662319085 | 0.002907656 | 0.048976629 |
| TCF21 | 3.189872 | 0.085908038 | -5.214561602 | 0.002869776 | 0.048976629 |
| MCM2 | 3.466193333 | 52.52739823 | 3.921646096 | 0.002969847 | 0.048976629 |
| CACNB2 | 3.546071333 | 0.143111465 | -4.631010398 | 0.002907656 | 0.048976629 |
| MAP6 | 3.770149333 | 0.232398213 | -4.019950787 | 0.002969847 | 0.048976629 |
| STARD8 | 4.046868 | 0.579137356 | -2.80482833 | 0.002969847 | 0.048976629 |
| DNAJC18 | 4.105557 | 0.851534115 | -2.269441731 | 0.002969847 | 0.048976629 |
| ABCA8 | 4.243906 | 0.104108682 | -5.34923041 | 0.002907415 | 0.048976629 |
| FEN1 | 4.245454 | 39.62434142 | 3.222396211 | 0.002907656 | 0.048976629 |
| AC005180.1 | 4.319371333 | 0.10970813 | -5.299079001 | 0.002676123 | 0.048976629 |
| PGM5P4 | 4.466981 | 0.061985645 | -6.171222156 | 0.001334966 | 0.048976629 |
| ABCC9 | 4.678883667 | 0.183156014 | -4.675019383 | 0.002969847 | 0.048976629 |
| C1QTNF7 | 4.795991667 | 0.163575051 | -4.873804526 | 0.002907556 | 0.048976629 |
| CKS1B | 4.879866667 | 27.9482614 | 2.517844905 | 0.002907656 | 0.048976629 |
| PLPP7 | 4.934464667 | 0.261087022 | -4.240290927 | 0.002907656 | 0.048976629 |
| REEP4 | 5.081881 | 42.67654261 | 3.070008805 | 0.002907656 | 0.048976629 |

Table I. Continued.

| Gene | Normal mean | Tumor mean | logFC | P-value | FDR |
|---|---|---|---|---|---|
| MCM5 | 5.320449333 | 29.57469622 | 2.474743353 | 0.002969847 | 0.048976629 |
| CMA1 | 5.378929667 | 0.078556297 | -6.097448395 | 0.002371218 | 0.048976629 |
| ZDHHC14 | 5.434402667 | 1.034312338 | -2.393449555 | 0.002969847 | 0.048976629 |
| AC027449.1 | 5.444661 | 0.096116507 | -5.823914194 | 0.002281905 | 0.048976629 |
| RNASEH2A | 5.474293 | 41.41412395 | 2.919378312 | 0.002907656 | 0.048976629 |
| AVPR1A | 5.481554 | 0.367751649 | -3.897781233 | 0.002969847 | 0.048976629 |
| KIF22 | 5.775282667 | 28.40978773 | 2.298424587 | 0.002907656 | 0.048976629 |
| HSPB2 | 5.852205333 | 0.270781266 | -4.433780553 | 0.002907556 | 0.048976629 |
| AC011472.4 | 5.928092667 | 0.389895757 | -3.92640764 | 0.002907599 | 0.048976629 |
| JPT1 | 6.380713667 | 63.13397343 | 3.306626852 | 0.002907656 | 0.048976629 |
| ALG3 | 6.436405333 | 24.27056442 | 1.914880572 | 0.002907656 | 0.048976629 |
| AL049838.1 | 6.503072333 | 0.420695562 | -3.950272966 | 0.002907556 | 0.048976629 |
| EBF1 | 6.611833667 | 0.442443688 | -3.901484679 | 0.002907656 | 0.048976629 |
| MEF2C | 6.728852667 | 0.705862737 | -3.252900965 | 0.002969847 | 0.048976629 |
| MYOCD | 6.996498667 | 0.102720679 | -6.089834575 | 0.002969601 | 0.048976629 |
| ZNF25 | 7.554867 | 1.683135292 | -2.166255211 | 0.002969847 | 0.048976629 |
| AL031429.2 | 7.769253533 | 0.031932759 | -7.926594995 | 0.002356484 | 0.048976629 |
| VEGFD | 7.808901333 | 0.171508728 | -5.508765681 | 0.002907025 | 0.048976629 |
| KIAA1522 | 7.813884333 | 51.56979363 | 2.722414467 | 0.002907656 | 0.048976629 |
| RECK | 8.13414 | 0.775032279 | -3.391661519 | 0.002969847 | 0.048976629 |
| CASQ2 | 8.312275667 | 0.121069969 | -6.101330542 | 0.002898258 | 0.048976629 |
| LEPR | 8.325784333 | 0.674650187 | -3.625374639 | 0.002969847 | 0.048976629 |
| TUBG1 | 8.337667667 | 29.424488 | 1.819301538 | 0.002969847 | 0.048976629 |
| TEK | 8.535434667 | 0.677732175 | -3.654677456 | 0.002969847 | 0.048976629 |
| KPNA2 | 8.540581333 | 67.03229788 | 2.972450212 | 0.002907656 | 0.048976629 |
| ACTA2-AS1 | 8.612886 | 0.24691938 | -5.124384757 | 0.002969847 | 0.048976629 |
| CCL14 | 8.827088333 | 0.121593624 | -6.181798153 | 0.002867082 | 0.048976629 |
| AC012085.2 | 8.845370333 | 0.072649553 | -6.927824818 | 0.002798703 | 0.048976629 |
| TCEAL6 | 8.920253 | 0.022519671 | -8.629755081 | 0.001402316 | 0.048976629 |
| PAFAH1B3 | 8.988921333 | 49.43504549 | 2.459314251 | 0.002969847 | 0.048976629 |
| AC053503.4 | 9.164009667 | 0.083320645 | -6.781161168 | 0.000164822 | 0.048976629 |
| GPIHBP1 | 9.366506667 | 0.134603951 | -6.120718419 | 0.002904384 | 0.048976629 |
| ATOH8 | 9.419009 | 0.448944619 | -4.390965884 | 0.002969847 | 0.048976629 |
| TRPC4 | 9.738115667 | 0.145428399 | -6.065261709 | 0.002969835 | 0.048976629 |
| ABCG2 | 10.176267 | 0.409445899 | -4.635391781 | 0.002907656 | 0.048976629 |
| LGI4 | 10.311944 | 0.601528799 | -4.099538714 | 0.002907656 | 0.048976629 |
| RANGAP1 | 10.32322533 | 44.33790046 | 2.102646666 | 0.002907656 | 0.048976629 |
| AP001107.5 | 10.62646067 | 0.253305039 | -5.390641573 | 0.002901848 | 0.048976629 |
| PDE2A | 10.95424967 | 0.494103392 | -4.470533898 | 0.002907656 | 0.048976629 |
| GPRASP1 | 11.455003 | 0.552640084 | -4.373493819 | 0.002907656 | 0.048976629 |
| MMRN1 | 12.15564167 | 0.522061313 | -4.541262989 | 0.002969847 | 0.048976629 |
| MYCT1 | 12.30727667 | 0.762555452 | -4.012525498 | 0.002969847 | 0.048976629 |
| TNXB | 12.857966 | 0.456718245 | -4.815214207 | 0.002907656 | 0.048976629 |
| SAMD1 | 13.00907 | 41.81634958 | 1.684549296 | 0.002969847 | 0.048976629 |
| SGCA | 13.19399167 | 0.197471119 | -6.062095624 | 0.002969788 | 0.048976629 |
| KCNJ8 | 13.53072233 | 0.921078094 | -3.876771568 | 0.002907656 | 0.048976629 |
| TIE1 | 13.80315467 | 1.427333232 | -3.273603931 | 0.002969847 | 0.048976629 |
| RHOJ | 13.874021 | 1.100021946 | -3.656781762 | 0.002969847 | 0.048976629 |
| HSPA12B | 14.034565 | 0.972455828 | -3.851207818 | 0.002907656 | 0.048976629 |
| FGF7 | 14.537865 | 0.520324267 | -4.804260609 | 0.002969844 | 0.048976629 |
| DBI | 15.14378 | 65.29300935 | 2.108203179 | 0.002907656 | 0.048976629 |
| FAM110D | 16.130117 | 0.720151257 | -4.485313138 | 0.002907656 | 0.048976629 |

Table I. Continued.

| Gene | Normal mean | Tumor mean | logFC | P-value | FDR |
|---|---|---|---|---|---|
| CNRIP1 | 16.31504667 | 0.989692338 | -4.043079194 | 0.002969847 | 0.048976629 |
| FRMD6-AS2 | 16.315638 | 0.070309123 | -7.858327798 | 0.001728836 | 0.048976629 |
| CXorf36 | 16.816334 | 0.861871217 | -4.286247105 | 0.002907656 | 0.048976629 |
| JAM2 | 17.52046 | 0.675551827 | -4.69683039 | 0.002907656 | 0.048976629 |
| CRY2 | 17.84693667 | 3.796723552 | -2.232849603 | 0.002969847 | 0.048976629 |
| MITF | 18.94895667 | 1.400401072 | -3.758206439 | 0.002907656 | 0.048976629 |
| ADGRL4 | 19.25257667 | 2.112064328 | -3.188325861 | 0.002969847 | 0.048976629 |
| JPH2 | 19.33681 | 0.772258646 | -4.646121884 | 0.002907656 | 0.048976629 |
| DACT3 | 19.65532333 | 0.624052469 | -4.977108954 | 0.002907656 | 0.048976629 |
| EMCN | 19.71717233 | 0.714594377 | -4.786184296 | 0.002907656 | 0.048976629 |
| MRVI1 | 20.67947667 | 1.229043436 | -4.072591867 | 0.002907656 | 0.048976629 |
| TCF23 | 20.77050833 | 0.096224314 | -7.753919336 | 0.002941943 | 0.048976629 |
| ADH1B | 21.589176 | 0.242721229 | -6.474864072 | 0.002935074 | 0.048976629 |
| PDZRN3 | 23.89231333 | 1.010759848 | -4.563034381 | 0.002969847 | 0.048976629 |
| MMRN2 | 24.07429333 | 2.602476773 | -3.209536258 | 0.002969847 | 0.048976629 |
| JAM3 | 24.25990667 | 1.557027809 | -3.961707384 | 0.002907656 | 0.048976629 |
| PCNA | 26.66728333 | 215.2883285 | 3.013127342 | 0.002907656 | 0.048976629 |
| LDB2 | 26.84531333 | 1.120228078 | -4.582805845 | 0.002969847 | 0.048976629 |
| SERTM1 | 27.00274533 | 0.295550294 | -6.513558623 | 0.002277432 | 0.048976629 |
| RAB3IL1 | 28.05983667 | 2.484895139 | -3.497249734 | 0.002969847 | 0.048976629 |
| ZCCHC12 | 32.23301333 | 0.38459773 | -6.389045008 | 0.002969204 | 0.048976629 |
| MXRA7 | 32.36333 | 4.08448121 | -2.986135309 | 0.002969847 | 0.048976629 |
| RASL12 | 35.02677333 | 1.685038159 | -4.377604925 | 0.002907656 | 0.048976629 |
| PPP1R12B | 36.13469 | 2.383394038 | -3.922295126 | 0.002907656 | 0.048976629 |
| PLAC9 | 36.57375667 | 1.376582116 | -4.731646243 | 0.002969847 | 0.048976629 |
| RAI2 | 38.13514 | 1.739924689 | -4.454024229 | 0.002907656 | 0.048976629 |
| CD34 | 38.94151 | 2.532088291 | -3.942909212 | 0.002907656 | 0.048976629 |
| PODN | 39.42252 | 1.995966966 | -4.303860252 | 0.002907656 | 0.048976629 |
| TBC1D1 | 39.68758333 | 6.338195114 | -2.646543739 | 0.002969847 | 0.048976629 |
| RERG | 45.54668667 | 1.610461774 | -4.821799786 | 0.002907656 | 0.048976629 |
| MSRB3 | 47.28062667 | 2.374195522 | -4.315738502 | 0.002907656 | 0.048976629 |
| C7 | 53.39584333 | 0.747076013 | -6.159328587 | 0.00296535 | 0.048976629 |
| CHRDL1 | 56.66380333 | 0.493004955 | -6.844681482 | 0.002945266 | 0.048976629 |
| TNS1 | 57.79483333 | 4.231390233 | -3.771736879 | 0.002969847 | 0.048976629 |
| GNG11 | 58.94997667 | 3.146258062 | -4.227782329 | 0.002907656 | 0.048976629 |
| PRELP | 63.81604667 | 3.606790139 | -4.145131851 | 0.002907656 | 0.048976629 |
| ITM2A | 63.81789667 | 4.108238425 | -3.957369243 | 0.002969847 | 0.048976629 |
| MATN2 | 65.18636667 | 6.405312375 | -3.34722943 | 0.002969847 | 0.048976629 |
| NDN | 69.41545667 | 3.558211637 | -4.286032714 | 0.002907656 | 0.048976629 |
| FBLN5 | 71.73318 | 4.392540344 | -4.029513146 | 0.002907656 | 0.048976629 |
| PLN | 74.64023 | 0.821842713 | -6.504947309 | 0.002907556 | 0.048976629 |
| CXCL12 | 76.48481333 | 2.589450314 | -4.884455536 | 0.002907656 | 0.048976629 |
| KANK2 | 91.52304 | 8.810647905 | -3.376814954 | 0.002969847 | 0.048976629 |
| PGM5-AS1 | 103.9762653 | 0.153204864 | -9.406576423 | 0.001700567 | 0.048976629 |

logFC, log fold change.

survival, the clinical data of CC from TCGA were utilized to analyze the survival of the driver genes and related methylated sites. The construction of Kaplan-Meier curves was conducted to identify the association between methylation-driven genes and the survival rate of patients with CC. The prognosis of patients with CC was predicted by identifying latent methylation-driven mRNAs and methylation-driven lncRNAs.

Table II. Methylation-driven lncRNAs.

| Gene | Normal mean | Tumor mean | logFC | P-value | Cor | Cor P-value |
|---|---|---|---|---|---|---|
| CTSK | 0.359953657 | 0.778931247 | 1.113684816 | 0.002907613 | -0.333186659 | 2.28E-09 |
| HMGA1 | 0.336366172 | 0.114271749 | -1.557563851 | 0.002907622 | -0.346189262 | 4.83E-10 |
| ZIK1 | 0.112378753 | 0.423256447 | 1.913162742 | 0.002907633 | -0.4225026 | 1.12E-14 |
| PTTG1 | 0.239439619 | 0.119640652 | -1.000954214 | 0.002969791 | -0.410831811 | 6.86E-14 |
| ZSCAN18 | 0.287461835 | 0.583381623 | 1.021069511 | 0.003033222 | -0.582416793 | 3.48E-29 |
| CDO1 | 0.143990529 | 0.567419479 | 1.978441762 | 0.003097858 | -0.381641109 | 4.78E-12 |
| F11R | 0.35962326 | 0.142571806 | -1.334797621 | 0.003097864 | -0.360185914 | 8.35E-11 |
| NOVA1 | 0.070986809 | 0.549410942 | 2.952262777 | 0.003163751 | -0.359827999 | 8.74E-11 |
| ZNF582 | 0.118658864 | 0.513854519 | 2.114540083 | 0.003197172 | -0.623223069 | 2.54E-34 |
| DDR2 | 0.380932141 | 0.789642763 | 1.051666101 | 0.003230892 | -0.317960483 | 1.29E-08 |
| CHMP4C | 0.347515219 | 0.162185406 | -1.099432153 | 0.00329935 | -0.391735829 | 1.15E-12 |
| ZNF677 | 0.084379051 | 0.573297327 | 2.764326789 | 0.003299369 | -0.602084535 | 1.44E-31 |
| PTPRD | 0.11697317 | 0.492863393 | 2.07501017 | 0.003440272 | -0.367446412 | 3.25E-11 |
| LAMA4 | 0.26922608 | 0.581786764 | 1.111672304 | 0.003738586 | -0.343996592 | 6.31E-10 |
| ZNF418 | 0.177561931 | 0.63031161 | 1.827742931 | 0.003738618 | -0.493238972 | 3.64E-20 |
| CDKN2A | 0.200931093 | 0.095506903 | -1.073023924 | 0.00397755 | -0.320163484 | 1.01E-08 |
| ARNTL2 | 0.366240185 | 0.155970223 | -1.231519468 | 0.00406028 | -0.321666208 | 8.53E-09 |
| GYPC | 0.238177584 | 0.602450285 | 1.338804554 | 0.004060299 | -0.449701958 | 1.22E-16 |
| ZNF790-AS1 | 0.039053506 | 0.358995752 | 3.200442814 | 0.004060303 | -0.579449912 | 7.72E-29 |
| ZNF135 | 0.284970925 | 0.679272407 | 1.253175522 | 0.004317812 | -0.654121773 | 9.58E-39 |
| AF186192.1 | 0.111066679 | 0.493975764 | 2.1530142 | 0.004497656 | -0.453585503 | 6.20E-17 |
| THSD7A | 0.100507008 | 0.537490751 | 2.418943824 | 0.004684211 | -0.430102805 | 3.29E-15 |
| LRFN5 | 0.08563937 | 0.514578088 | 2.587043942 | 0.00478012 | -0.356743502 | 1.30E-10 |
| SPARCL1 | 0.221767893 | 0.687152496 | 1.631579789 | 0.004877773 | -0.409453404 | 8.46E-14 |
| ZNF880 | 0.045439117 | 0.424736649 | 3.224561903 | 0.005286769 | -0.611950539 | 7.93E-33 |
| PABPC1P4 | 0.344094877 | 0.688325541 | 1.000284629 | 0.005958452 | -0.668913704 | 4.72E-41 |
| CPXM2 | 0.235657194 | 0.503267657 | 1.094636163 | 0.006575888 | -0.40452501 | 1.78E-13 |
| ANGPTL1 | 0.224534915 | 0.735755194 | 1.712286021 | 0.006838515 | -0.372454964 | 1.67E-11 |
| HENMT1 | 0.234654382 | 0.106237576 | -1.143243265 | 0.007536963 | -0.389308525 | 1.63E-12 |
| ZNF471 | 0.069975202 | 0.453574624 | 2.696424276 | 0.00783384 | -0.690878505 | 9.82E-45 |
| EMX2 | 0.098532812 | 0.321111542 | 1.704398389 | 0.007986166 | -0.338378799 | 1.24E-09 |
| CTTNBP2 | 0.072730113 | 0.167092872 | 1.200025464 | 0.00845908 | -0.329763608 | 3.40E-09 |
| FAXDC2 | 0.168151612 | 0.364885714 | 1.117682056 | 0.008459093 | -0.378660562 | 7.20E-12 |
| CLSTN2 | 0.142064024 | 0.409902778 | 1.528740508 | 0.009128618 | -0.318465241 | 1.22E-08 |
| ROR2 | 0.060251887 | 0.132899666 | 1.141259162 | 0.015707688 | -0.33512759 | 1.82E-09 |
| SLIT2 | 0.156368293 | 0.407988703 | 1.383581202 | 0.020261048 | -0.42849441 | 4.27E-15 |
| PREX2 | 0.08137986 | 0.399527012 | 2.295549348 | 0.020261061 | -0.364080516 | 5.05E-11 |
| CTSK | 0.359953657 | 0.778931247 | 1.113684816 | 0.002907613 | -0.333186659 | 2.28E-09 |

logFC, log fold change; Cor, correlation.

*Bisulfite sequencing for the determination of Fms related receptor tyrosine kinase 1 (FLT1) methylation*. The methylation status of the FLT1 promoter was determined using bisulfite sequencing. DNA was extracted and digested with EcoRV (Takara Bio, Inc.). The EpiTect Bisulite Kit (Qiagen, Inc.) was used to perform the bisulfite sequencing analysis with the EpiTect Bisulite kit (Qiagen, Inc.) according to the manufacturer's instructions. The transformed DNA was then PCR-amplified using the Takara Taq kit (Takara Bio, Inc.). The sequences of the primers used are presented in Table SI. The KK8504 kit (Kapa Biosystems, Inc.) was used for DNA library construction for each sample and for sequencing on Nova-seq6000 (Illumina, Inc.). A total of 12 clinical samples, including 10 cervical cancer specimens and 2 normal cervical specimens were randomly selected for this FLT1 methylation assay. The clinical features of the 10 cervical cancer samples are listed in Table SII. Ethical approval was obtained from the Ethics Committee of the Affiliated Hospital of Qingdao University. Two cervical cancer tissue samples were excluded due to quality problems. Finally, four squamous cell

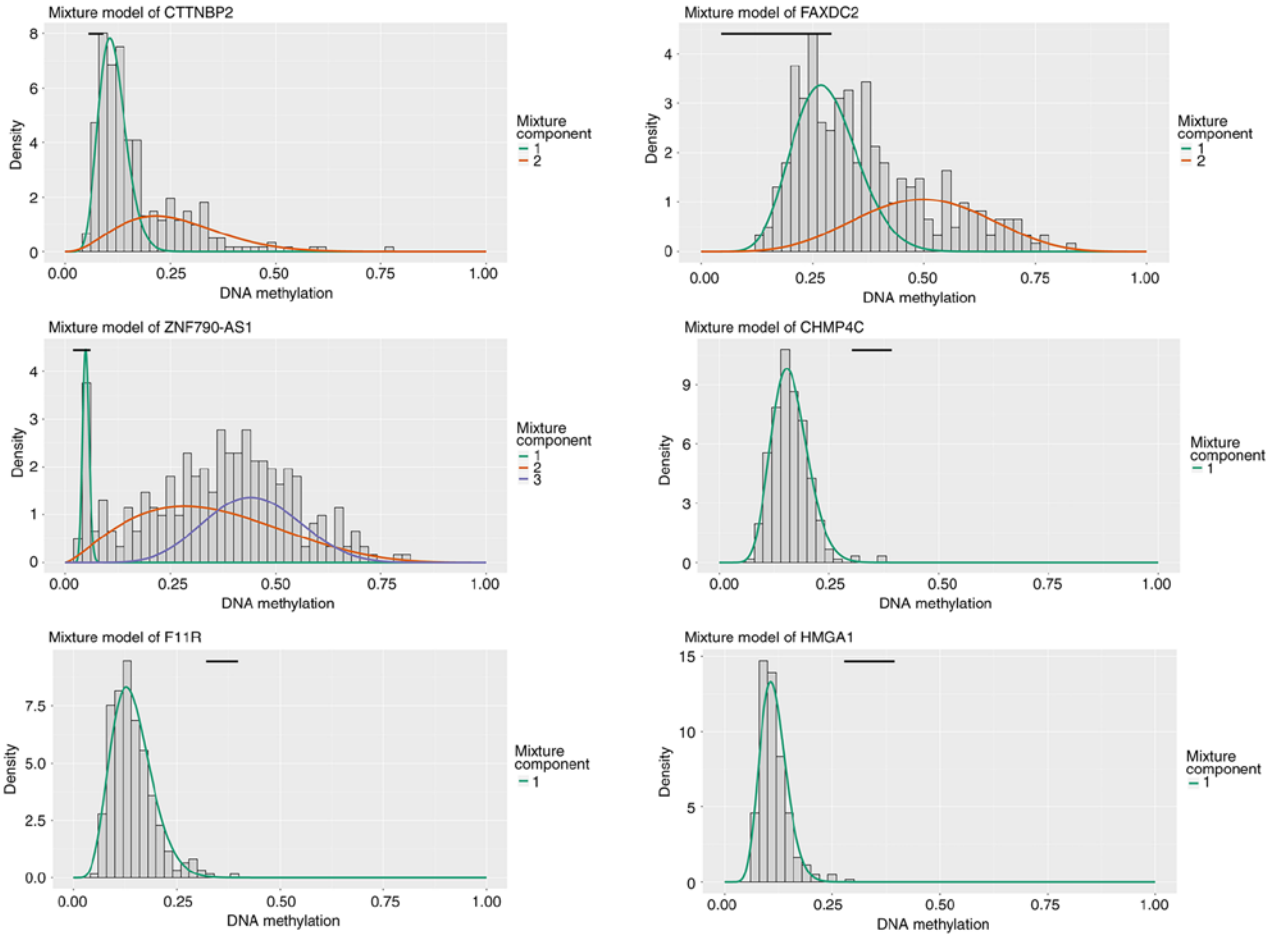


Figure 1. MethylMix model of DNA methylation-driven genes. (A) The distribution maps illustrate the methylation states of methylated genes. The X-axis represents the degree of methylation and the Y-axis represents the number of methylated samples; the black horizontal line represents the methylation degree distribution in normal samples.

carcinoma, four adenocarcinoma and two normal cervical tissues were collected for detection.

*Immunohistochemical analysis*. A total of 25 paraffin-embedded CC tissue specimens and 15 paraffin-embedded normal cervical epithelium tissue specimens were collected from The Affiliated Hospital of Qingdao University. The present study was approved by the Institutional Review Board of the Affiliated Hospital of Qingdao University Health Science Center Ethics Committee (approval no. QYFY WZLL 25964). All patients or their patents/guardians in the present study provided written informed consent for participation in the study. The clinical parameters of the 25 patients with CC are presented in Table SII. CC tissue specimens embedded in paraffin were cut into 3- to 5-$\mu$m-thick serial sections and fixed onto slides. The sections were then deparaffinized in xylene twice for 10 min, and rehydrated through graded ethanol to distilled water. After conducting antigen retrieval with a microwave for 5 min at 95˚C, endogenous peroxidase activity and non-specific binding activity were blocked with 3% hydrogen peroxide and 5% non-fat dried milk, respectively. Subsequently, the sections were incubated with anti-human FLT1 (AF321, R&D Systems, Inc.) and PLEKHG6 antibodies (PA5-59578, Thermo Fisher Scientific, Inc.) overnight at 4˚C in a humidified chamber. The primary antibodies were replaced by immunoglobulin (Rabbit Immunoglobulin Fraction, #X0936; Agilent Technologies, Inc.) for the negative control. The following day, sections were incubated with horseradish peroxidase-labeled anti-goat IgG secondary antibody (CST Inc., Danvers, MA, USA.) at room temperature for 30 min. Finally, slides were visualized by 3,3-diaminobenzidine (DAB) staining.

*Statistical analysis*. The R statistical package (R version 3.6.2) and SPSS 23.0 software (SPSS, Inc.) were used for statistical analysis. The Student's t-test was used for comparing the methylation status of FLT1 between the groups.

## Results

*Identification of methylation-driven mRNAs and lncRNAs in CC*. DNA methylation data were extracted from 309 cervical cancer specimens, including 3 normal samples and 306 tumor samples. Using the cut-off criteria of a false discovery rate (FDR) <0.05 and logFC >1, a total of 2,916 DEGs were screened for further analysis. The gene expression data and DNA methylation data for the 2,916 DEGs were included in the MethylMix analysis with a screening criteria set as |logFC|>1, P<0.05 and Cor <-0.3. In total, 200 mRNAs and 38 lncRNAs were identified for DNA methylation in virtue of

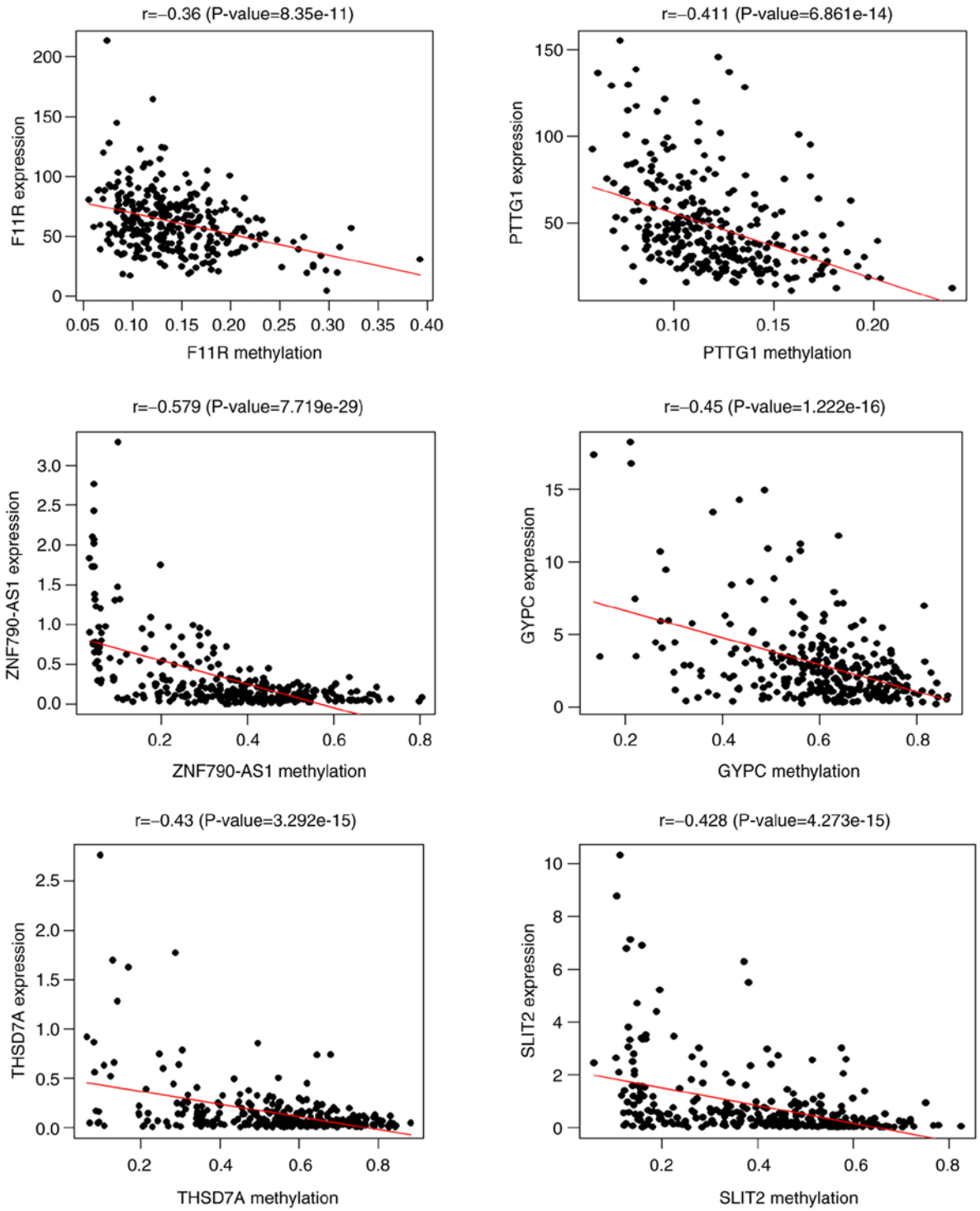


Figure 2. Correlation between the expression levels of selective genes and the degree of methylation. Pearson's correlation analysis revealed a negative correlation between gene expression and methylation for F11R, PTTG1, ZNF790-AS1, GYPC, THSD7A and SLIT2. The X-axis represents the methylation degree and the Y-axis represents the gene expression level. r represents the correlation coefficient of Pearson's analysis.

the MethylMix criteria. The methylation-driven mRNAs and lncRNAs are listed in Tables I and II, respectively. As shown in Fig. 1, the distributed area of the methylation degree indicated that CTTNBP2, FAXDC2, ZNF790-AS1, CHMP4C, F11R and HMGA1 were hypermethylated in patients with CC and hypomethylated in non-CC patients. Pearson's correlation analysis revealed a negative correlation between the gene expression and methylation of F11R, PTTG1, ZNF790-AS1, GYPC, THSD7A, and SLIT2 (Fig. 2). The expression patterns and methylation values of the methylation-driven genes are illustrated as a heatmap in Fig. 3.

*Enrichment analysis of methylation-driven mRNAs in CC.* According to the results of the GO enrichment analysis, there were eight GO terms with statistically significant differences ($P<0.05$): Synaptic membrane adhesion, heterochromatin assembly, heterochromatin organization, positive regulation of cellular senescence, positive regulation of cell aging, cell-cell

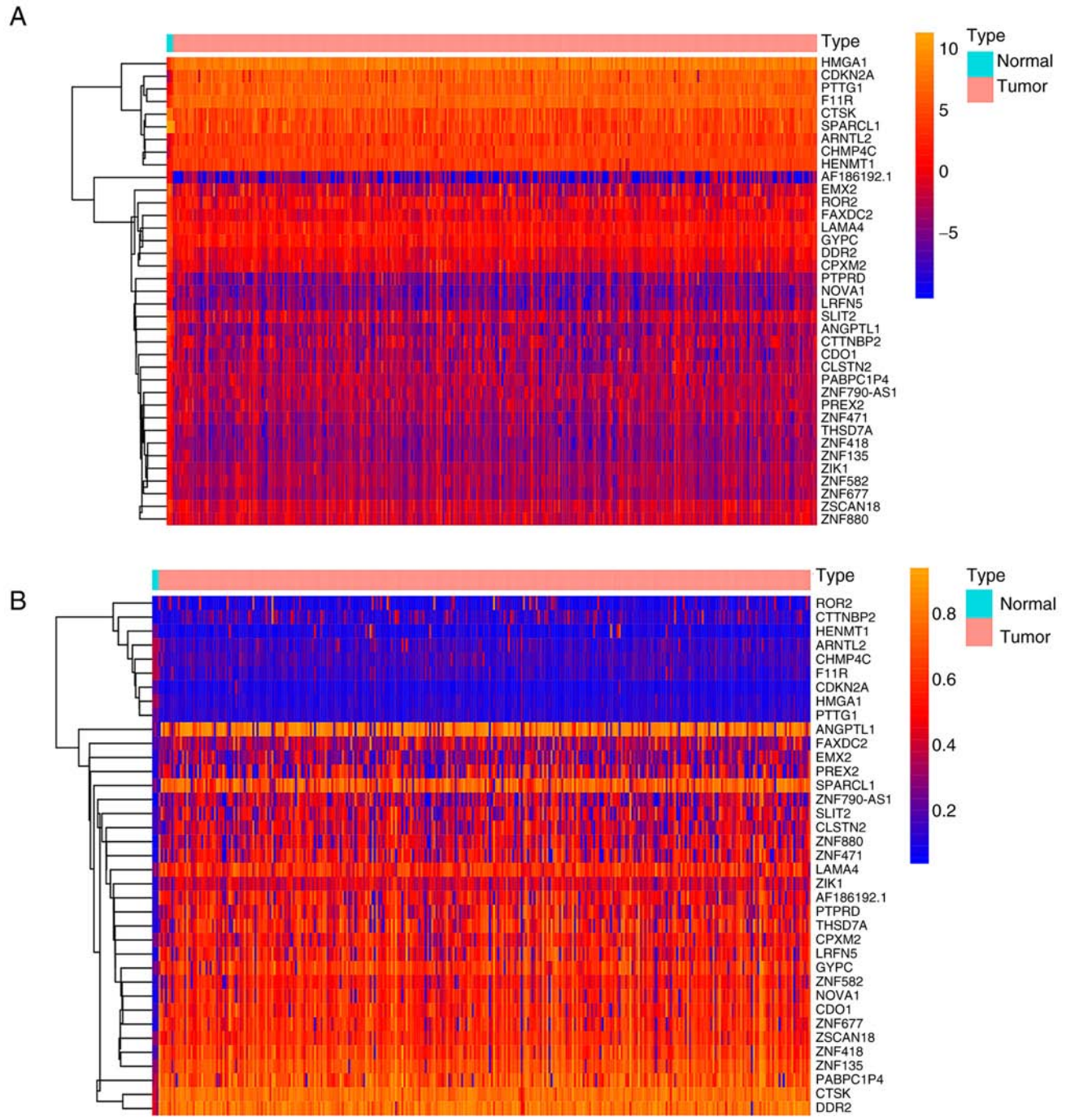


Figure 3. Heatmap of 37 methylation-driven genes in cervical cancer. (A) Expression patterns of 37 methylation-driven genes. The orange-red color represents upregulated genes and blue represents downregulated genes between tumor and normal tissues. (B) Methylation patterns of 37 methylation-driven genes. Orange red represents highly methylated genes and blue represents low methylated genes between tumor and normal tissues.

adhesion via plasma-membrane adhesion molecules, regulation of presynapse assembly, and the regulation of presynapse organization. 'GO:0099560 synaptic membrane adhesion' exhibited the highest GO biological process (Fig. 4A). As shown in Fig. 4B, three pathways (hsa05168, hsa00430 and hsa04110) were regarded to be of statistical significance ($P<0.05$); the highest KEGG pathway was 'hsa05168 Herpes simplex virus 1 infection'.

*Establishment of a predictive model of two distinctively methylated lncRNAs in CC*. The univariate Cox regression model was conducted for identifying the prognosis in relevance to differentially methylated genes in CC and incorporated three methylation genes conspicuous relevance to the overall survival rate ($P<0.05$). The univariate and multivariate Cox regression model revealed that two lncRNAs were eventually related to the survival rate of patients with CC (Tables III and IV).

*Analysis of risk groupings and ROC curve*. Based on the median risk scores, a total of 304 samples of complete survival information were classified into a high-risk group (n=152) and low-risk group (n=152). The risk score of the low-risk group was

Table III. Univariate Cox regression analysis of two lncRNAs associated with overall survival in patients with cervical cancer.

| Genes | HR | 95% CI of HR | P-value |
|---|---|---|---|
| FLT1 | 0.153 | 0.0266-0.876 | 0.035 |
| MKI67 | 7622606324559.52 | 3137.628-1.851E+22 | 0.007 |

HR, hazard ratio; CI, confidence interval.

Table IV. Multivariate Cox regression analysis of two lncRNAs associated with the overall survival of patients with cervical cancer.

| Genes | HR | 95% CI of HR | P-value |
|---|---|---|---|
| FLT1 | 0.158 | 0.0280-0.894 | 0.037 |
| MKI67 | 9.805E+12 | 3111.326-3.09E+22 | 0.007 |

HR, hazard ratio; CI, confidence interval.

in the range of 0.5 to 1.0; 1.0 to 2.5 was the risk score attached to the high-risk group with rapid growth trends (Fig. 5A). The distributions of risk scores and the OS status of each patient are illustrated in Fig. 5B, suggesting a good discrimination between the low- and high-risk groups. The Kaplan-Meier curve based on the log-rank statistical examination was used for survival analysis. Patients with CC belonging to the low-risk group exhibited an improved OS compared with those in the high-risk group (P<0.001) (Fig. 5C). According to the heatmap, the expression of two prognostic methylation genes was profiled (Fig. 5D). ROC curve analysis further revealed an excellent prediction efficiency with an AUC value of 0.816 (Fig. 5E).

*Combined methylation and gene expression survival analysis in CC*. In accordance with the combined Kaplan-Meier curve analysis, the combined methylation and mRNA presentation of FLT1 was relevant to the OS rate of patients with CC (P=0.036; Fig. 6A). The low expression of FLT1 with hypermethylation was associated with a higher survival rate as compared with the high expression of FLT1 with hypomethylation. The combination methylation and presentation of the lncRNAs marker of proliferation Ki-67 (MKI67), PLEKHG6 and DNA polymerase epsilon 2, accessory subunit (POLE2) harbored a marked relevance to the prognosis of patients with CC (P=0.021, 0.015 and 0.022, respectively) (Fig. 6B-D).

*Promoter methylation level of FLT1 in CC tissues*. The methylation levels of the FLT1 promoter were significantly higher in tumor tissue than in normal tissue (CC: 27.9±8.8, P=0.0008; cervical squamous carcinoma: 22.9±14.1, P=0.048; cervical adenocarcinoma: 28.6±1.9, P=0.0005) (Fig. 7A-C). The volcano plot revealed DNA methylation differences of the FLT1 promoter in CC tissues. Compared with the normal tissue group, 52 of the CpGs were hypermethylated in the adenocarcinoma group (Fig. 7D) and eight of the CpGs were hypermethylated in the squamous carcinoma group (Fig. 7E). The methylation values of the FLT1 promoter are presented as a heatmap in Fig. 7F and G).

*Validation of FLT1 and PLEKHG6 expression*. The results of the staining of normal cervical tissues demonstrated that FLT1 was negatively expressed in normal cervical tissues (Fig. 8A). As regards FLT1, the staining was low, and the intensity was weak in stage II cervical adenocarcinoma (Fig. 8A). FLT1 was highly expressed in stage III/IV cervical adenocarcinoma (Fig. 8A). However, as regards PLEKHG6 (Fig. 8B), when compared with normal cervical tissues (Fig. 8B), staining was not detected, and the intensity was negative in stage II/III/IV cervical adenocarcinoma tissues (Fig. 8B).

## Discussion

As precise medicine is developing rapidly, the further discovery of diagnostic and prognostic biomarkers is of utmost urgency in order to enhance the decision making for CC. Over the years, it has been found that the decreased expression of genes caused by hypomethylation plays a crucial role in the regulating and developing malignant tumors. Abnormal DNA methylation is an effective tumor marker (25,26), which can lead to the inactivation of tumor suppressor genes, interference with genomic imprinting and genomic instability by reducing the formation of heterochromatin on repeat sequences (27). A number of studies have revealed that tumor formation is intimately associated with aberrant DNA methylation, which can alter the expression of proto-oncogenes and tumor suppressor genes (28-30). The present study identified abnormal gene methylation by comparing normal and CC samples using MethyMix. To further explore the functions of the DNA methylation-driven genes identified, GO and KEGG pathway enrichment analyses were performed. DNA methylation driven gene function was enriched in molecular functions, including immune receptor activity, cytokine activity and cytokine receptor binding. Function analysis and pathway analysis revealed that the function of these genes could regulate tumor cell migration, metabolism and the cell cycle.

DNA methylation is known as a type of covalent modification of DNA. The primary mechanism through which epigenetic modification modulates genomic function is related to the regulation of the expression of multiple differentiation-related genes in mammals (31,32). In terms of high-activity promoters with a vast range of CpG islands, on a general basis, disease-associated or experimental methylation will lead to the alteration of transcription factor interaction and histone modification, as well as the *cis*-silencing of previously active genes (33). Zhong and Cen (27) proved that the abnormality of promoter methylation was closely related to the survival and prognosis of patients with hepatic carcinoma. Moreover, the function could silence certain tumor suppressor genes and other key genes which can mediate cellular signaling pathways in cancerous tissues (27). Dong *et al* (34) concluded that the promoter methylations of RASSF1A, BVES and HOXA9 in combination with serum alpha fetoprotein was associated with a marked improvement in the diagnosis of patients with hepatitis B-associated hepatocellular carcinoma (34). According

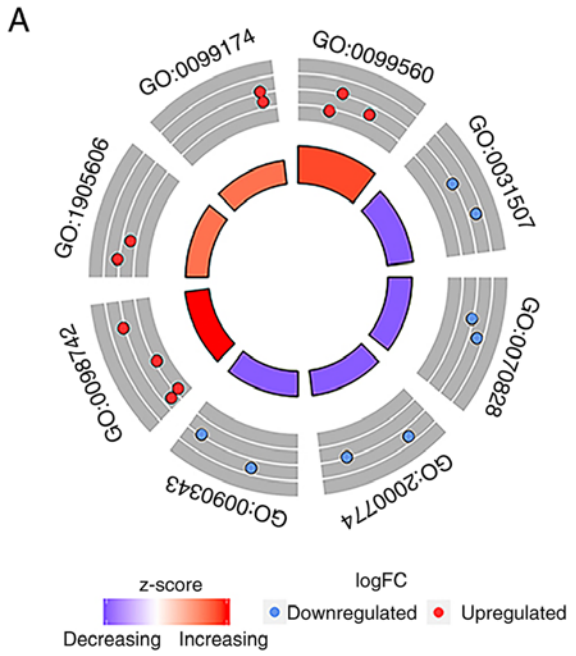


| ID | Description |
|---|---|
| GO:0099560 | synaptic membrane adhesion |
| GO:0031507 | heterochromatin assembly |
| GO:0070828 | heterochromatin organization |
| GO:2000774 | positive regulation of cellular senescence |
| GO:0090343 | positive regulation of cell aging |
| GO:0098742 | cell–cell adhesion via plasma–membrane adhesion molecules |
| GO:1905606 | regulation of presynapse assembly |
| GO:0099174 | regulation of presynapse organization |

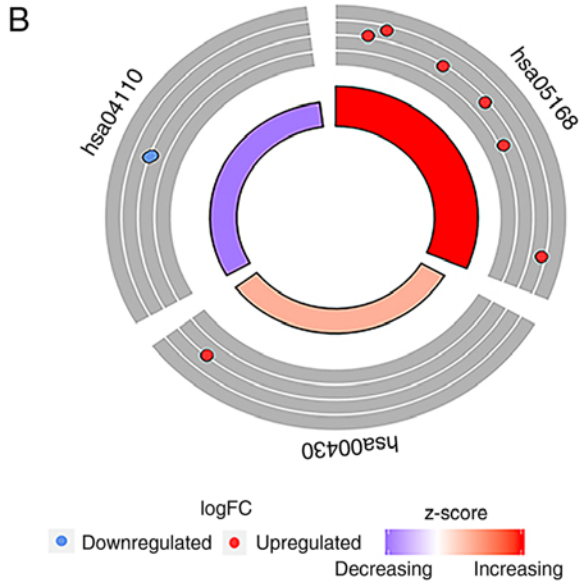


| ID | Description |
|---|---|
| hsa05168 | Herpes simplex virus 1 infection |
| hsa00430 | Taurine and hypotaurine metabolism |
| hsa04110 | Cell cycle |

Figure 4. Functional enrichment analysis of methylation-driven genes in cervical cancer. (A) Gene ontology analysis of methylation-driven genes of cervical cancer. (B) Pathway analysis of methylation-driven genes of cervical cancer. The color of the inner circle represents the Z score, while the band thickness of the inner circle represents the significance of GO terms ($log_{10}$-adjusted P-values). The outer circle represents the expression ($log_2$FC) of methylation-driven mRNAs in each enriched GO term: Red dots indicate upregulated methylation-driven mRNAs, while blue dots indicate downregulated methylation-driven mRNAs. GO, Gene Ontology.

to the downregulation of tumor-repressing genes and key molecules modulating cellular signaling pathways associated with promoter methylation, promoter hypermethylation can suppress the expression of liver cancer genes, which is negatively associated with gene expression in normal and tumor tissues (25,32,35). Recent studies on the effects of lncRNAs in tumorigenesis and metastasis have demonstrated that lncRNAs may become potential novel biomarkers for the diagnosis and prognosis of cancers (27,36,37). For example, lncRNA PVT1, as a promising serum biomarker associated with CC detection, has been shown to facilitate CC progression by negatively regulating miR-424 (38). As also previously demonstrated, the hypomethylation of the lncRNA SOX21-AS1 may function as a clinical prognostic indicator in CC (39). lncRNA NEAT1 has also been shown to accelerate CC growth by sponging miR-9-5p (40). Another study also demonstrated that lncRNA HOXD-AS1 regulated CC proliferation by modulating the Ras/ERK signaling pathway (41).

In the present study, one mRNA and three lncRNAs were identified as independent prognostic factors for the monitoring and prognosis of CC by combining methylation, mRNA and lncRNA expression data with survival analysis. Joint survival analysis demonstrated that the low expression of FLT1 with hypermethylation was associated with a higher survival rate than the high expression of FLT1 with hypomethylation. Compared with a high expression with hypomethylation, the

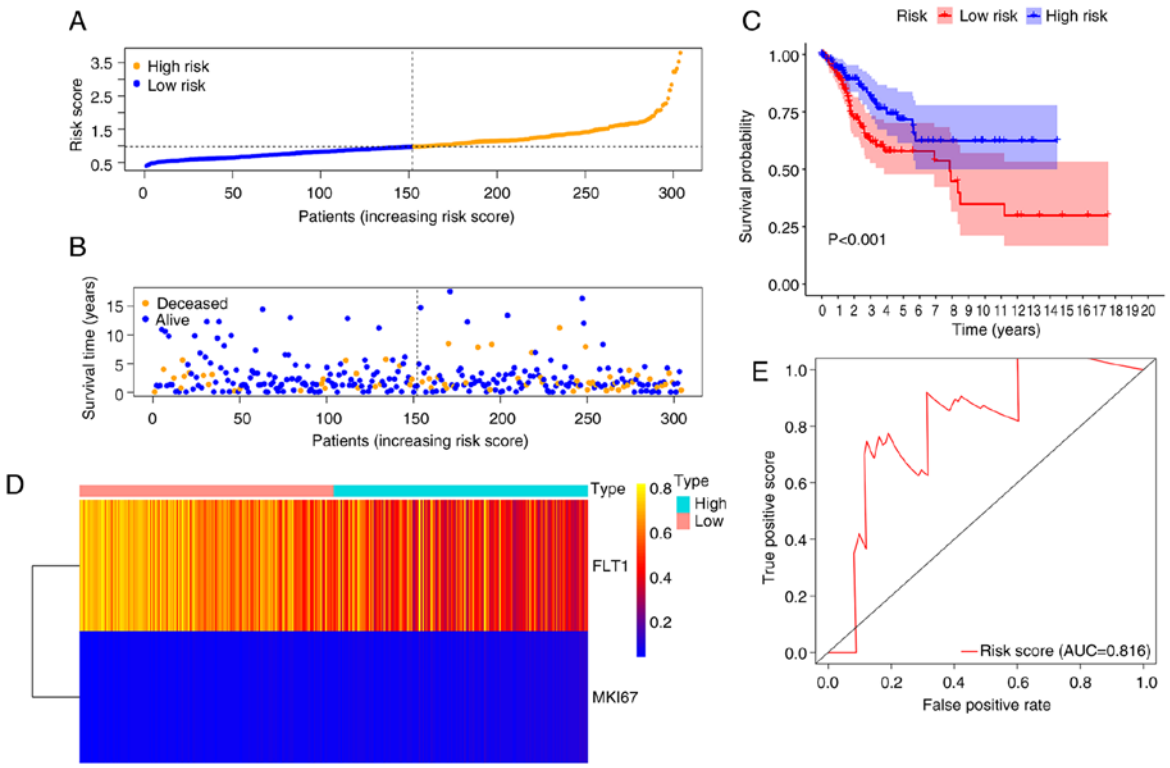


Figure 5. Validation of the prognostic risk signature. (A) The distributions of risk scores of patients. (B) The distributions of risk scores and overall survival status. (C) The survival analysis of the two subgroups stratified based on the median of risk scores. (D) The expression pattern of the two methylation-driven genes in low and high-risk groups. (E) ROC curve for evaluating the prediction efficiency of the prognostic signature.

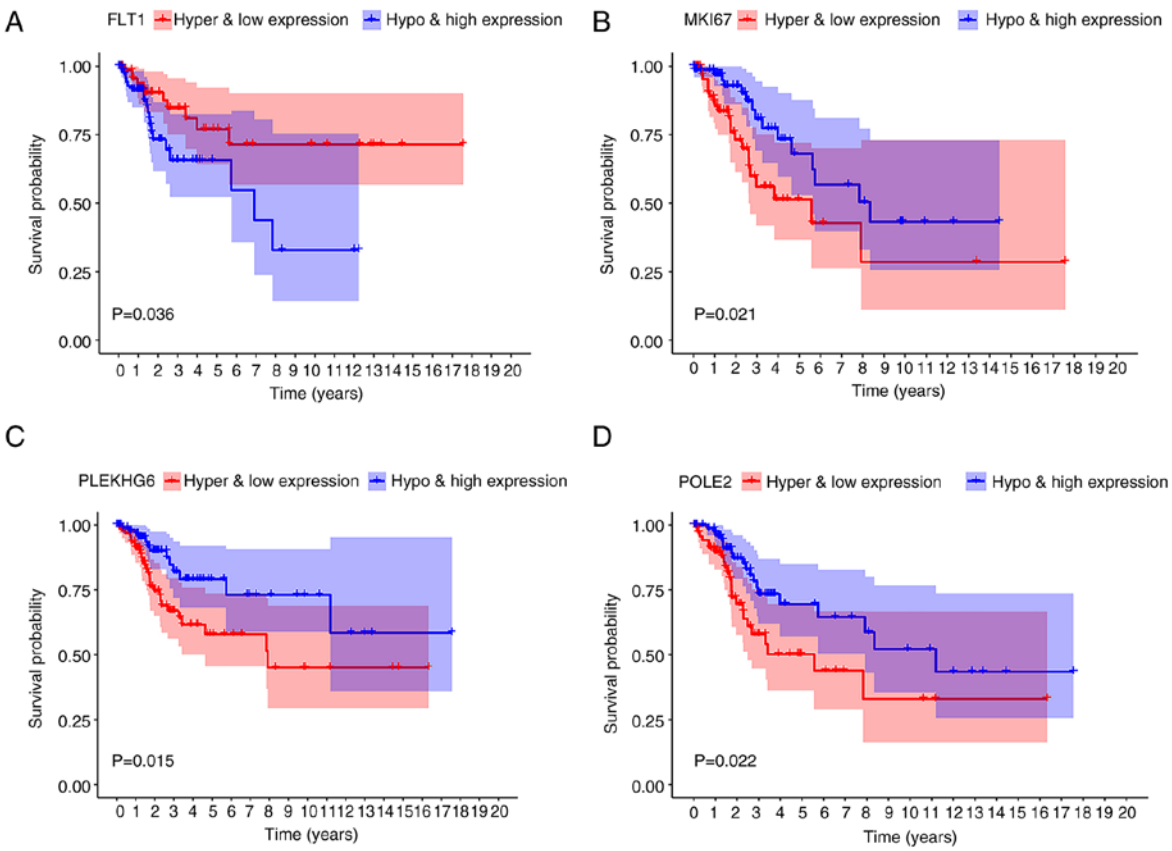


Figure 6. Kaplan-Meier survival curves for joint survival analysis. (A) Combination of FLT1 gene methylation and expression. (B) Combination of MKI67 gene methylation and expression. (C) Combination of PLEKHG6 gene methylation and expression. (D) Combination of POLE2 gene methylation and expression. FLT1, Fms related receptor tyrosine kinase 1; MKI67, marker of proliferation Ki-67; PLEKHG6, pleckstrin homology and RhoGEF domain containing G6; POLE2, DNA polymerase epsilon 2, accessory subunit.

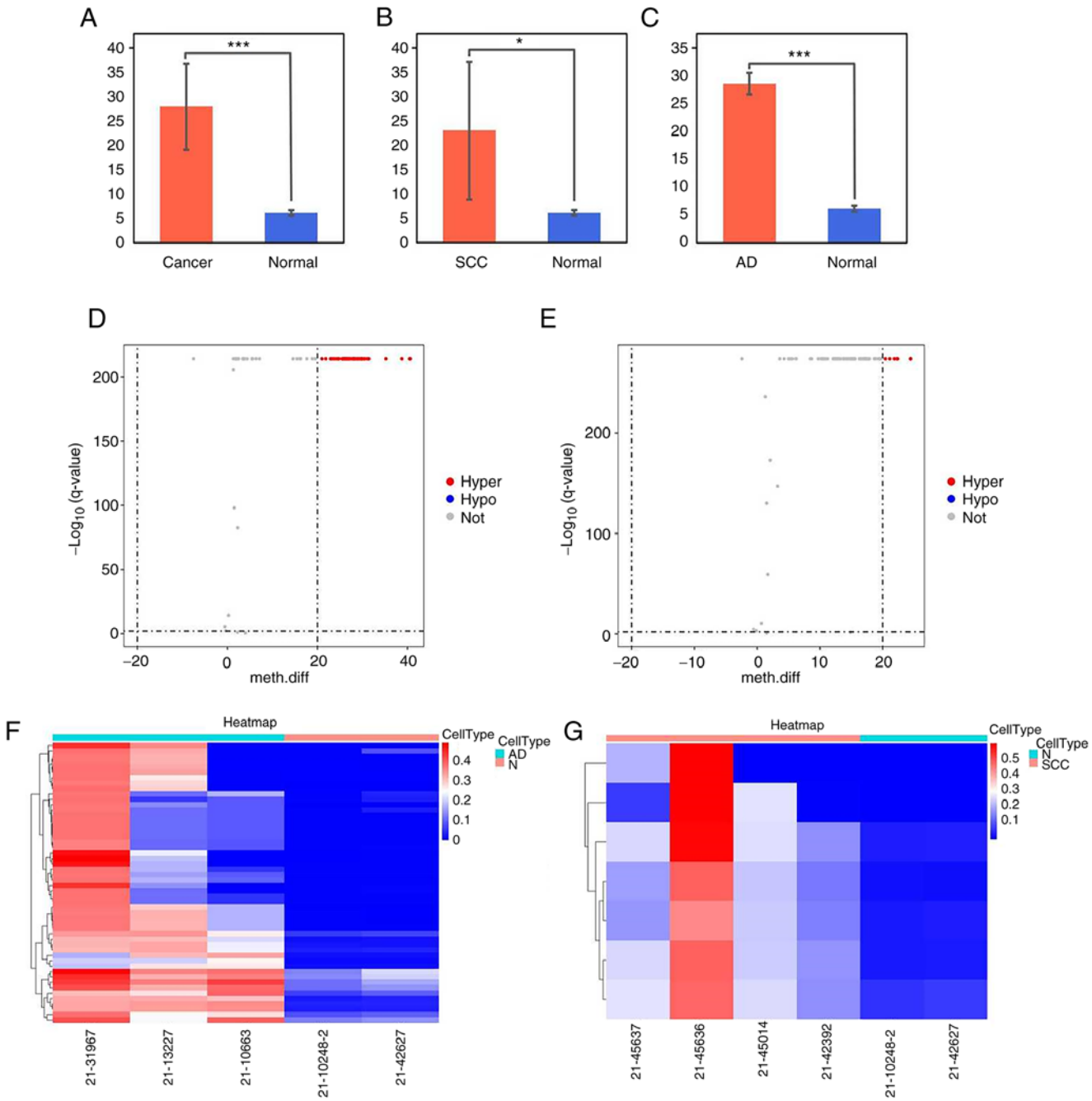


Figure 7. Methylation status of FLT1 promoter from cervical cancer clinical samples. (A) Methylation levels in normal and cervical cancer group (***P<0.01). (B) Methylation levels in normal and cervical adenocarcinoma group (*P<0.05). (C) Methylation levels in normal and cervical squamous carcinoma group (***P<0.01). (D) Volcano plot illustrating DNA methylation differences of the FLT1 promoter in adenocarcinoma tissues. (E) Volcano plot illustrating DNA methylation differences of the FLT1 promoter in squamous carcinoma tissues. (F) The methylation values of FLT1 promoter in adenocarcinoma tissues are presented as a heatmap. (G) The methylation values of the FLT1 promoter in squamous carcinoma tissues are presented as a heatmap. FLT1, Fms related receptor tyrosine kinase 1.

low expression of MKI67, PLEKH6 and POLE2 with hypermethylation was associated with a lower survival rate. As a result, lncRNA MKI67, PLEKHG6 and POLE2 may function as cancer suppressor genes under the regulation of DNA methylation, playing crucial roles in predicting the prognosis of CC.

FLT1 (VEGFR1) is a tyrosine kinase receptor with a binding affinity to VEGF-A ~10-fold higher than other kinase insert domain receptors, and it is associated with tumor growth and metastasis (42). FLT1 activation upgrades epithelial-mesenchymal transition, as well as an aggressive phenotype in specific cancer cells (43). Promoter hypermethylation is known to play a key role in the epigenetic silencing of tumor suppressor genes in the development and progression of cancers (44). The expression level of FLT1 in individual tissues of patients with CC differs. Therefore, FLT1 may function as a potential biomarker for the monitoring and prognosis of patients with CC. In the present study, the promoter methylation levels of FLT1 were significantly upregulated in cervical squamous cell carcinoma and adenocarcinoma compared with normal controls. This result is consistent with the findings

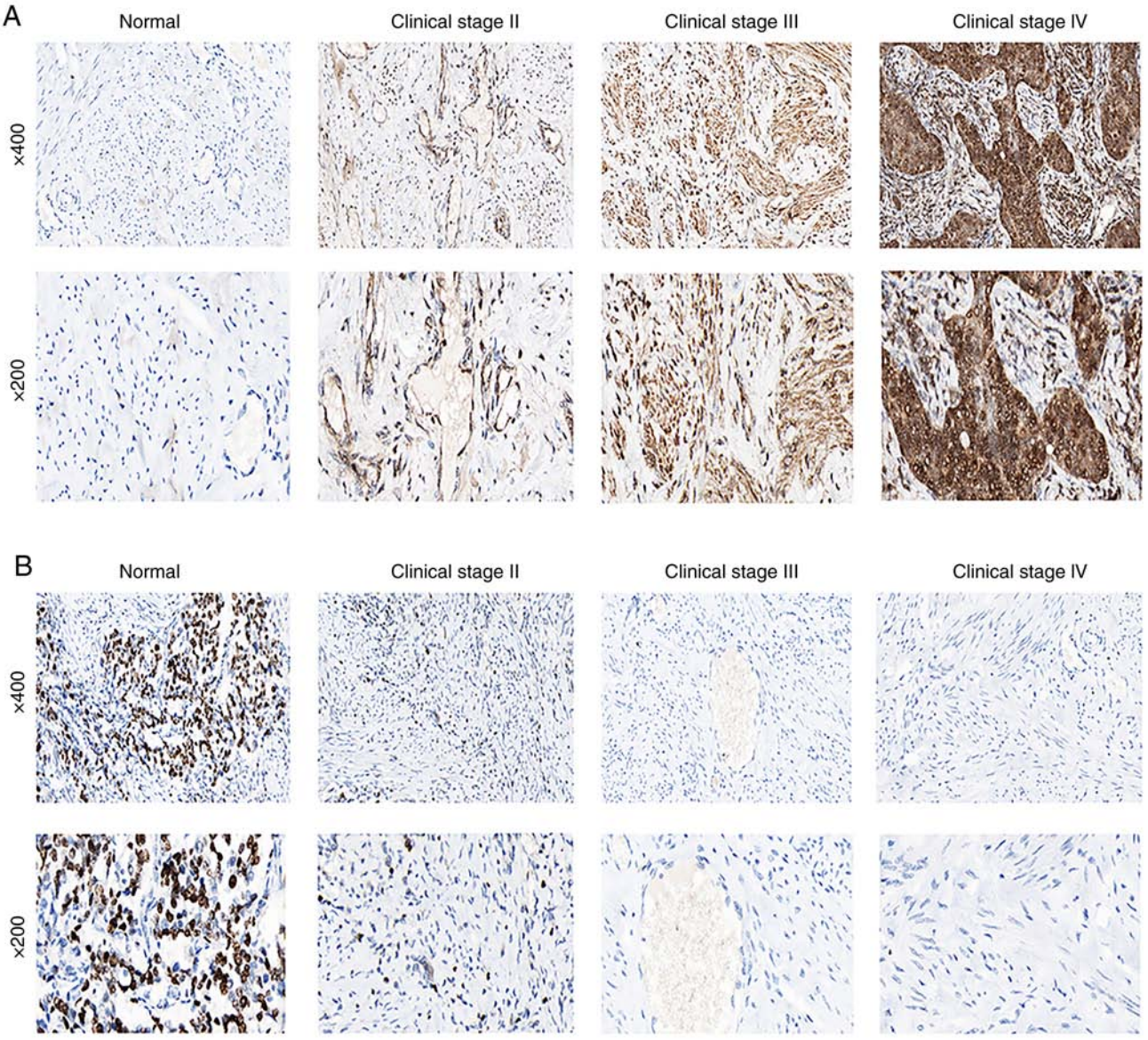


Figure 8. Validation of FLT1 and PLEKHG6 expression in human cervical cancer tissues. Compared with normal cervical tissues, the results of stains demonstrated that (A) FLT1 was highly expressed in high cervical adenocarcinoma (stage II/III/IV); (B) PLEKHG6, compared with normal tissues, the results demonstrated that no staining was detected, and the staining intensity was negative in stage II/III/IV cervical adenocarcinoma, respectively. FLT1, Fms related receptor tyrosine kinase 1; PLEKHG6, pleckstrin homology and RhoGEF domain containing G6.

of another previous experimental study on head and neck squamous cell carcinoma (HNSCC), suggesting that the methylation levels of the FLT1 promoter tended to be higher in HNSCC than in normal tonsil samples (45). Methylation of the FLT1 promoter has also been found to be significantly higher in tumor tissues of prostate cancer, renal cancer, and chorio carcinoma, in comparison with normal tissues (46-48). In the present study, Kaplan-Meier analysis revealed that the hypomethylation of FLT1 with a low expression predicted a longer survival of patients with CC. The results revealed that FLT1 was upregulated and was associated with a poor prognosis (Fig. 6). However, the experimental results demonstrated that its expression was not inversely correlated with DNA methylation in CC tissues (Figs. 7 and 8). This inconsistency may be due to the expression levels determined and the cervical tissues used in DNA methylation analysis were not from the same patients or controls. Another possible explanation for this is that the immunohistochemistry method on tissue sample is a semi-quantitative method, thus not highly informative. In the present study, FLT1 protein expression was not quantified; therefore, further studies are required for validation. The methylation status of the FLT1 promoter may be useful as a novel potential biomarker for CC diagnosis. The authors aim to continue to detect FLT1 methylation using more samples in future studies to confirm the accuracy of the findings presented herein.

The nuclear staining of the nuclear antigen Ki-67 has the most popular application as an agent oriented with multiplication activity. Ki-67 exists within the cell nucleus all through cell-cycle stages which excluded the resting phase G0. MKI67 protein is employed as a proliferation-oriented biomarker for determining benign, malignant tumors, or the malignancy-oriented histological grade. The percentage of Ki-67-expressing cells (Ki-67 labeling index) is used for

assessing the multiplication of neoplastic cells, as this increases in separating cells, culminating in cells in the M phase (49-51). Song *et al* (52) revealed that hypomethylation may contribute to the overexpression of MKI67 in breast cancer and may lead to the pathological process of breast cancer. In addition, a previous meta-analysis demonstrated that a high expression level of MKI-67 led to the poor overall survival, as well as illness-free survival of patients with colorectal cancer (53). The present study demonstrated that the high methylation level of MKI67 was associated with a lower survival ratio of patients with CC. This may provide a novel treatment strategy and may also aid in improving the prognosis of patients with CC.

A previous study indicated that a high PLEKHG6 expression was related to a shorter survival time of patients with colorectal cancer (54). A few studies have examined the gene PLEKHG6 (55-57). The present study demonstrated the potential of this gene as a novel target for the monitoring and prognosis of patients with CC. The present study revealed that PLEKHG6 expression was lower in cervical adenocarcinoma compared with adjacent para-carcinoma tissues using immunohistochemical analysis. It was previously reported that POLE2 is expressed in breast cancer, colorectal cancer, cervical and bladder cancer (58-61). Li *et al* (62) reported that lung adenocarcinoma cell malignant phenotypes were suppressed by the knockdown of POLE2 expression. The present study found the POLE2 gene to be a renown prognostic-related methylation-driven genes in the CC group; the Kaplan-Meier curve revealed that patients with POLE2 hypermethylation had a lower survival rate and a shorter methylation survival period, which was confirmed by the combined survival analysis.

Some limitations of the present study need to be acknowledged. First, the present study was based only on research data from TCGA, which may contribute to selection bias. Second, the sample size of normal controls in TCGA was relatively small, and only three non-CC patients were included for analysis from the database. Third, FLT1 protein expression was not quantified. Therefore, further studies are warranted for experimental validation.

In conclusion, based on the genomic methylation data provided by TCGA for patients with CC, 48 methylation-driven genes associated with CC were obtained through the MethylMix algorithm. Univariate and multivariate Cox regression models revealed that the prognostic survival model constructed from four aberrant methylation-driven genes, including FLT1, MKI67, PLEKHG6 and POLE2, was an independent predictor for the prognosis of patients with CC. Based on the risk model of these five methylation-driven genes, patients with CC could be divided into a high- and a low-risk group, which provides a basis for prognosis prediction and personalized treatment plans. The expression levels of the genes, FLT1, MKI67, PLEKHG6 and POLE2, may be used as independent prognostic indicators for CC. Although further experimental verification is needed, the findings presented herein provide the bioinformatic and theoretical basis for guiding the subsequent in-depth study of CC.

## Acknowledgements

Not applicable.

## Funding

The present study was supported by the Chinese Postdoctoral Science Foundation (grant no. 88014Y0181).

## Availability of data and materials

The datasets used and/or analyzed during the current study are available from the corresponding author on reasonable request.

## Authors' contributions

BL, TZ and HL wrote the manuscript. BL, YL, TZ and HL performed the experiments. BL and BH analyzed the data. FC and QL designed the experiments and revised the manuscript. BL and FC confirm the authenticity of all the raw data. All authors have read and approved the final manuscript.

## Ethics approval and consent to participate

The present study was approved by the Institutional Review Board of the Affiliated Hospital of Qingdao University Health Science Center Ethics Committee (approval no. QYFY WZLL 25964). All patients or their patents/guardians in the present study provided written informed consent for participation in the study.

## Patient consent for publication

Not applicable.

## Competing interests

The authors declare that they have no competing interests.

## References

1. Arbyn M, Weiderpass E, Bruni L, de Sanjosé S, Saraiya M, Ferlay J and Bray F: Estimates of incidence and mortality of cervical cancer in 2018: A worldwide analysis. Lancet Glob Health 8: e191-e203, 2020.
2. Torre LA, Islami F, Siegel RL, Ward EM and Jemal A: Global cancer in women: Burden and trends. Cancer Epidemiol Biomarkers Prev 26: 444-457, 2017.
3. Jürgenliemk-Schulz IM, Beriwal S, de Leeuw AAC, Lindegaard JC, Nomden CN, Pötter R, Tanderup K, Viswanathan AN and Erickson B: Management of nodal disease in advanced cervical cancer. Semin Radiat Oncol 29: 158-165, 2019.
4. Mohan G and Chattopadhyay S: Cost-effectiveness of leveraging social determinants of health to improve breast, cervical, and colorectal cancer screening: A systematic review. JAMA Oncol 6: 1434-1444, 2020.
5. Bogani G, Maggiore ULR, Signorelli M, Martinelli F, Ditto A, Sabatucci I, Mosca L, Lorusso D and Raspagliesi F: The role of human papillomavirus vaccines in cervical cancer: Prevention and treatment. Crit Rev Oncol Hematol 122: 92-97, 2018.
6. Marlow LAV, Chorley AJ, Haddrell J, Ferrer R and Waller J: Understanding the heterogeneity of cervical cancer screening non-participants: Data from a national sample of British women. Eur J Cancer 80: 30-38, 2017.
7. Santoni G, Morelli MB, Amantini C and Battelli N: Urinary markers in bladder cancer: An update. Front Oncol 8: 362, 2018.
8. Sproul D, Kitchen RR, Nestor CE, Dixon JM, Sims AH, Harrison DJ, Ramsahoye BH and Meehan RR: Tissue of origin determines cancer-associated CpG island promoter hypermethylation patterns. Genome Biol 13: R84, 2012.

9. Heery R and Schaefer MH: DNA methylation variation along the cancer epigenome and the identification of novel epigenetic driver events. Nucleic Acids Res 49: 12692-12705, 2021.
10. Klutstein M, Nejman D, Greenfield R and Cedar H: DNA methylation in cancer and aging. Cancer Res 76: 3446-3450, 2016.
11. Moore LD, Le T and Fan G: DNA methylation and its basic function. Neuropsychopharmacology 38: 23-38, 2013.
12. Easwaran HP, Van Neste L, Cope L, Sen S, Mohammad HP, Pageau GJ, Lawrence JB, Herman JG, Schuebel KE and Baylin SB: Aberrant silencing of cancer-related genes by CpG hypermethylation occurs independently of their spatial organization in the nucleus. Cancer Res 70: 8015-8024, 2010.
13. Bogdanović O and Lister R: DNA methylation and the preservation of cell identity. Curr Opin Genet Dev 46: 9-14, 2017.
14. Clarke MA, Luhn P, Gage JC, Bodelon C, Dunn ST, Walker J, Zuna R, Hewitt S, Killian JK, Yan L, *et al*: Discovery and validation of candidate host DNA methylation markers for detection of cervical precancer and cancer. Int J Cancer 141: 701-710, 2017.
15. Yue Y, Zhou K, Li J, Jiang S, Li C and Men H: MSX1 induces G0/G1 arrest and apoptosis by suppressing Notch signaling and is frequently methylated in cervical cancer. Onco Targets Ther 11: 4769-4780, 2018.
16. Liu J, Nie S, Li S, Meng H, Sun R, Yang J and Cheng W: Methylation-driven genes and their prognostic value in cervical squamous cell carcinoma. Ann Transl Med 8: 868, 2020.
17. Yu J, Xie Y, Liu Y, Wang F, Li M and Qi J: MBD2 and EZH2 regulate the expression of SFRP1 without affecting its methylation status in a colorectal cancer cell line. Exp Ther Med 20: 242, 2020.
18. Hall CL, Bafico A, Dai J, Aaronson SA and Keller ET: Prostate cancer cells promote osteoblastic bone metastases through Wnts. Cancer Res 65: 7554-7560, 2005.
19. Planutiene M, Planutis K and Holcombe RF: Lymphoid enhancer-binding factor 1, a representative of vertebrate-specific Lef1/Tcf1 sub-family, is a Wnt-beta-catenin pathway target gene in human endothelial cells which regulates matrix metalloproteinase-2 expression and promotes endothelial cell invasion. Vasc Cell 3: 28, 2011.
20. Guo YH, Wang LQ, Li B, Xu H, Yang JH, Zheng LS, Yu P, Zhou AD, Zhang Y, Xie SJ, *et al*: Wnt/β-catenin pathway transactivates microRNA-150 that promotes EMT of colorectal cancer cells by suppressing CREB signaling. Oncotarget 7: 42513-42526, 2016.
21. Liu Z, Wan Y, Yang M, Qi X, Dong Z, Huang J and Xu J: Identification of methylation-driven genes related to the prognosis of papillary renal cell carcinoma: A study based on the cancer genome atlas. Cancer Cell Int 20: 235, 2020.
22. Lv L, Cao L, Hu G, Shen Q and Wu J: Methylation-driven genes identified as novel prognostic indicators for thyroid carcinoma. Front Genet 11: 294, 2020.
23. Han P, Liu Q and Xiang J: Monitoring methylation-driven genes as prognostic biomarkers in patients with lung squamous cell cancer. Oncol Lett 19: 707-716, 2020.
24. Lando M, Fjeldbo CS, Wilting SM, Snoek BC, Aarnes EK, Forsberg MF, Kristensen GB, Steenbergen RD and Lyng H: Interplay between promoter methylation and chromosomal loss in gene silencing at 3p11-p14 in cervical cancer. Epigenetics 10: 970-980, 2015.
25. Feinberg AP: Phenotypic plasticity and the epigenetics of human disease. Nature 447: 433-440, 2007.
26. Wang N, Wang J, Meng X, Li T, Wang S and Bao Y: The Pharmacological effects of spatholobi caulis tannin in cervical cancer and its precise therapeutic effect on related circRNA. Mol Ther Oncolytics 14: 121-129, 2019.
27. Zhong D and Cen H: Aberrant promoter methylation profiles and association with survival in patients with hepatocellular carcinoma. Onco Targets Ther 10: 2501-2509, 2017.
28. Cui J, Yin Y, Ma Q, Wang G, Olman V, Zhang Y, Chou WC, Hong CS, Zhang C, Cao S, *et al*: Comprehensive characterization of the genomic alterations in human gastric cancer. Int J Cancer 137: 86-95, 2015.
29. Nones K, Waddell N, Song S, Patch AM, Miller D, Johns A, Wu J, Kassahn KS, Wood D, Bailey P, *et al*: Genome-wide DNA methylation patterns in pancreatic ductal adenocarcinoma reveal epigenetic deregulation of SLIT-ROBO, ITGA2 and MET signaling. Int J Cancer 135: 1110-1118, 2014.
30. Wang G, Luo X, Wang J, Wan J, Xia S, Zhu H, Qian J and Wang Y: MeDReaders: A database for transcription factors that bind to methylated DNA. Nucleic Acids Res 46: D146-D151, 2018.
31. Rasmussen KD and Helin K: Role of TET enzymes in DNA methylation, development, and cancer. Genes Dev 30: 733-750, 2016.
32. Jones PA and Liang G: Rethinking how DNA methylation patterns are maintained. Nat Rev Genet 10: 805-811, 2009.
33. Yang X, Gao L and Zhang S: Comparative pan-cancer DNA methylation analysis reveals cancer common and specific patterns. Brief Bioinform 18: 761-773, 2017.
34. Dong X, Hou Q, Chen Y and Wang X: Diagnostic value of the methylation of multiple gene promoters in serum in hepatitis B virus-related hepatocellular carcinoma. Dis Markers 2017: 2929381, 2017.
35. Long J, Chen P, Lin J, Bai Y, Yang X, Bian J, Lin Y, Wang D, Yang X, Zheng Y, *et al*: DNA methylation-driven genes for constructing diagnostic, prognostic, and recurrence models for hepatocellular carcinoma. Theranostics 9: 7251-7267, 2019.
36. Bhan A, Soleimani M and Mandal SS: Long noncoding RNA and cancer: A new paradigm. Cancer Res 77: 3965-3981, 2017.
37. Yu J, Wu X, Huang K, Zhu M, Zhang X, Zhang Y, Chen S, Xu X and Zhang Q: Bioinformatics identification of lncRNA biomarkers associated with the progression of esophageal squamous cell carcinoma. Mol Med Rep 19: 5309-5320, 2019.
38. Chang QQ, Chen CY, Chen Z and Chang S: LncRNA PVT1 promotes proliferation and invasion through enhancing Smad3 expression by sponging miR-140-5p in cervical cancer. Radiol Oncol 53: 443-452, 2019.
39. Wang R, Li Y, Du P, Zhang X, Li X and Cheng G: Hypomethylation of the lncRNA SOX21-AS1 has clinical prognostic value in cervical cancer. Life Sci 233: 116708, 2019.
40. Xie Q, Lin S, Zheng M, Cai Q and Tu Y: Long noncoding RNA NEAT1 promotes the growth of cervical cancer cells via sponging miR-9-5p. Biochem Cell Biol 97: 100-108, 2019.
41. Hu YC, Wang AM, Lu JK, Cen R and Liu LL: Long noncoding RNA HOXD-AS1 regulates proliferation of cervical cancer cells by activating Ras/ERK signaling pathway. Eur Rev Med Pharmacol Sci 21: 5049-5055, 2017.
42. Wei SC, Liang JT, Tsao PN, Hsieh FJ, Yu SC and Wong JM: Preoperative serum placenta growth factor level is a prognostic biomarker in colorectal cancer. Dis Colon Rectum 52: 1630-1636, 2009.
43. Han L, Husaiyin S, Ma C, Wang L and Niyazi M: TNFAIP8L1 and FLT1 polymorphisms alter the susceptibility to cervical cancer amongst uyghur females in China. Biosci Rep 39: BSR20191155, 2019.
44. Wang YQ, Li YM, Li X, Liu T, Liu XK, Zhang JQ, Guo JW, Guo LY and Qiao L: Hypermethylation of TGF-β1 gene promoter in gastric cancer. World J Gastroenterol 19: 5557-5564, 2013.
45. Misawa Y, Misawa K, Kawasaki H, Imai A, Mochizuki D, Ishikawa R, Endo S, Mima M, Kanazawa T, Iwashita T and Mineta H: Evaluation of epigenetic inactivation of vascular endothelial growth factor receptors in head and neck squamous cell carcinoma. Tumour Biol 39: 1010428317711657, 2017.
46. Yamada Y, Watanabe M, Yamanaka M, Hirokawa Y, Suzuki H, Takagi A, Matsuzaki T, Sugimura Y, Yatani R and Shiraishi T: Aberrant methylation of the vascular endothelial growth factor receptor-1 gene in prostate cancer. Cancer Sci 94: 536-539, 2003.
47. Kim JY, Hwang J, Lee SH, Lee HJ, Jelinek J, Jeong H, Lim JS, Kim JM, Song KS, Kim BH, *et al*: Decreased efficacy of drugs targeting the vascular endothelial growth factor pathway by the epigenetic silencing of FLT1 in renal cancer cells. Clin Epigenetics 7: 99, 2015.
48. Sasagawa T, Jinno-Oue A, Nagamatsu T, Morita K, Tsuruga T, Mori-Uchino M, Fujii T and Shibuya M: Production of an anti-angiogenic factor sFLT1 is suppressed via promoter hypermethylation of FLT1 gene in choriocarcinoma cells. BMC Cancer 20: 112, 2020.
49. Soliman NA and Yussif SM: Ki-67 as a prognostic marker according to breast cancer molecular subtype. Cancer Biol Med 13: 496-504, 2016.
50. Li R, Heydon K, Hammond ME, Grignon DJ, Roach M III, Wolkov HB, Sandler HM, Shipley WU and Pollack A: Ki-67 staining index predicts distant metastasis and survival in locally advanced prostate cancer treated with radiotherapy: An analysis of patients in radiation therapy oncology group protocol 86-10. Clin Cancer Res 10: 4118-4124, 2004.
51. Wong E, Nahar N, Hau E, Varikatt W, Gebski V, Ng T, Jayamohan J and Sundaresan P: Cut-point for Ki-67 proliferation index as a prognostic marker for glioblastoma. Asia Pac J Clin Oncol 15: 5-9, 2019.

52. Song B, Wang L, Zhang Y, Li N, Dai H, Xu H, Cai H and Yan J: Combined detection of HER2, Ki67, and GSTP1 genes on the diagnosis and prognosis of breast cancer. Cancer Biother Radiopharm 34: 85-90, 2019.
53. Zhang SD, McCrudden CM, Meng C, Lin Y and Kwok HF: The significance of combining VEGFA, FLT1, and KDR expressions in colon cancer patient prognosis and predicting response to bevacizumab. Onco Targets Ther 8: 835-843, 2015.
54. Zhang P, Ma Y, Wang F, Yang J, Liu Z, Peng J and Qin H: Comprehensive gene and microRNA expression profiling reveals the crucial role of hsa-let-7i and its target genes in colorectal cancer metastasis. Mol Biol Rep 39: 1471-1478, 2012.
55. O'Neill AC, Kyrousi C, Klaus J, Leventer RJ, Kirk EP, Fry A, Pilz DT, Morgan T, Jenkins ZA, Drukker M, *et al*: A primate-specific isoform of PLEKHG6 regulates neurogenesis and neuronal migration. Cell Rep 25: 2729-2741, 2018.
56. D'Angelo R, Aresta S, Blangy A, Del Maestro L, Louvard D and Arpin M: Interaction of ezrin with the novel guanine nucleotide exchange factor PLEKHG6 promotes RhoG-dependent apical cytoskeleton rearrangements in epithelial cells. Mol Biol Cell 18: 4780-4793, 2007.
57. Jiao M, Wu D and Wei Q: Myosin II-interacting guanine nucleotide exchange factor promotes bleb retraction via stimulating cortex reassembly at the bleb membrane. Mol Biol Cell 29: 643-656, 2018.
58. Wu Z, Wang YM, Dai Y and Chen LA: POLE2 Serves as a prognostic biomarker and is associated with immune infiltration in squamous cell lung cancer. Med Sci Monit 26: e921430, 2020.
59. Rogers RF, Walton MI, Cherry DL, Collins I, Clarke PA, Garrett MD and Workman P: CHK1 inhibition is synthetically lethal with loss of B-family DNA polymerase function in human lung and colorectal cancer cells. Cancer Res 80: 1735-1747, 2020.
60. Liu D, Zhang XX, Xi BX, Wan DY, Li L, Zhou J, Wang W, Ma D, Wang H and Gao QL: Sine oculis homeobox homolog 1 promotes DNA replication and cell proliferation in cervical cancer. Int J Oncol 45: 1232-1240, 2014.
61. Zekri AR, Hassan ZK, Bahnassy AA, Khaled HM, El-Rouby MN, Haggag RM and Abu-Taleb FM: Differentially expressed genes in metastatic advanced Egyptian bladder cancer. Asian Pac J Cancer Prev 16: 3543-3549, 2015.
62. Li J, Wang J, Yu J, Zhao Y, Dong Y, Fan Y, Li N, Zhang Y and Wang Y: Knockdown of POLE2 expression suppresses lung adenocarcinoma cell malignant phenotypes *in vitro*. Oncol Rep 40: 2477-2486, 2018.